Multipartite quantum nonlocality and Bell-type inequalities in a spin-1/2 model with topological quantum phase transitions

Zhao-Yu Sun,[1,*] Hui-Xin Wen,[1] Meng Li,[1] and Yuebin Li[2]

[1]*School of Electrical and Electronic Engineering, Wuhan Polytechnic University, Wuhan 430023, China*
[2]*Hubei Key Laboratory of Ferro and Piezoelectric Materials and Devices,Faculty of Physics and Electronic Sciences, Hubei University, Wuhan 430062, China*

Multipartite quantum nonlocality and Bell-type inequalities are used to characterize quantum correlations in an infinite-size bond-alternating spin-$\frac{1}{2}$ Heisenberg chain with next-nearest-neighbor interactions. With the help of powerful tensor-network algorithms, both zero and finite temperatures are considered. First, at zero temperature, both in the even-Haldane phase and in the odd-Haldane phase, a high hierarchy of multipartite nonlocality is observed. Nevertheless, in the two phases, the spread of the multipartite nonlocality among the lattice is different. Thereby, the nonlocality measures are relatively large in one phase and vanish in the other phase, and provide quite sharp signals for the topological quantum phase transitions (QPTs) between these two phases. The influence of the next-nearest-neighbor coupling α upon the multipartite nonlocality in the model is also discussed. Second, we find that the footprints of the QPTs survive at low temperatures. Third, based upon the scaling behavior of the finite-temperature nonlocality measure, we propose a quantity $\mathcal{K}$ to characterize the finite-temperature nonlocality in the large-n limit. We find that in high-temperature regions, $\mathcal{K}$ is reduced linearly as the temperature rises.

I. INTRODUCTION

Bipartite quantum entanglement (such as entanglement entropy and entanglement concurrence) has been widely investigated in the fields of quantum information and condensed matter physics for many years [1,2]. As the research goes deeper, it is realized that bipartite entanglement cannot capture all the characteristics of quantumness in quantum systems [3–6]. Recently, based upon Bell-type inequalities, multipartite quantum nonlocality has been proposed to characterize multipartite quantum correlations in many-body systems [7–12]. Since it can reveal some valuable information beyond bipartite entanglement, multipartite nonlocality has attracted much attention [13–19].

In the field of condensed matter physics, an important application for multipartite nonlocality is to characterize quantum phase transitions (QPTs) [20]. QPTs occur at zero temperature. When a physical parameter λ of a quantum system (such as the magnetic field in a quantum magnetic system) changes, the ground state of the system may be in various quantum phases. At some point $\lambda = \lambda_c$, the ground state drastically changes from a phase to another, then a QPT occurs. Characterization of these quantum phases and corresponding QPTs is one of the most important topics in condensed matter physics. There are several traditional approaches to characterize QPTs, such as local order parameters and symmetry breaking. However, when multipartite nonlocality is used to characterize these QPTs, some interesting

results are found [21–27]. For instance, it is observed that these QPTs are accompanied by a dramatic change of the *hierarchy* of multipartite nonlocality. In addition, it is also observed that the boundary effect of multipartite nonlocality in the vicinity of the QPT point is quite different from that in noncritical regions [28]. Thereby, multipartite nonlocality indeed provides a valuable perspective for us to understand and characterize QPTs.

In addition to traditional QPTs, recently a novel family of QPTs has attracted much attention, that is, the nonlocal topological QPTs [29–32]. Different from traditional QPTs, topological QPTs could not be characterized by local order parameters or symmetry breaking. Thereby, various advanced approaches and tools, which originate from quite different areas, have been used to characterize these topological QPTs, for instance, the global flux [33], Chern number [34], Wigner-Yanase skew information [35], topological entanglement entropy [36,37], quantum fidelity [38], and nonlocal string orders [39–43].

It needs to be mentioned that multipartite nonlocality, which can measure multipartite quantum correlations in n-site systems, would spontaneously have a nonlocal nature when n is large enough. Thus, multipartite nonlocality may capture the underlying changes of the topological orders in the systems and detect these topological QPTs. In a pioneering work, Deng *et al.* [44] have investigated quantum nonlocality in the Kitaev-Castelnovo-Chamon (KCC) model and have found that the nonlocality measure is singular at the topological QPT point. A spin-$\frac{1}{2}$ Kitaev chain has also been investigated recently, and the result suggests that the nonlocality measure may be used as an order parameter for the topological QPT

----
*Corresponding author: sunzhaoyu2020@whpu.edu.cn

in the chain [45]. Nevertheless, it is still too early to say that we have built a complete physical picture of the issue. For instance, in Ref. [44], only two-site subchains are considered and quantum nonlocality is actually not observed. In Ref. [45], the authors mainly consider thermal states ($T > 0$) rather than the ground states ($T = 0$), and the concerned state is the mixed state of low-lying energy states. Consequently, quantum correlations are destroyed by thermodynamic fluctuations and only the lowest hierarchy of multipartite nonlocality has been observed. Thereby, the role of multipartite nonlocality in topological QPTs is still not fully understood.

In this paper, based upon powerful tensor-network algorithms [46], we will investigate multipartite nonlocality in an infinite-size bond-alternating spin-$\frac{1}{2}$ Heisenberg chain with next-nearest-neighbor interactions. The model exhibits topological QPTs between an odd-Haldane phase and an even-Haldane phase. We will show that by analyzing the multipartite nonlocality measures, quite sharp signals for the topological QPTs are observed. Explicitly, where odd-bond subchains are concerned, in the odd-Haldane phase, a high hierarchy of multipartite nonlocality can be observed, while in most regions of the even-Haldane phase, the nonlocality measure is simply zero. The opposite result would be observed where even-bond subchains are concerned. Moreover, these footprints of the QPTs survive at low temperatures $T \gtrsim 0$. Furthermore, in high-temperature regions, a quantitative analysis about the effect of thermodynamic fluctuation upon multipartite nonlocality in the model will also be reported.

This paper is organized as follows. We will introduce the concepts of multipartite nonlocality and Bell-type inequalities in Sec. II. The model and the numerical details of the tensor-network solutions will be introduced in Sec. III. Our results for zero temperature and finite temperatures will be reported in Secs. IV and V, respectively. A summary and some discussions can be found in Sec. VI.

II. MULTIPARTITE NONLOCALITY AND BELL-TYPE INEQUALITIES

A. *g*-grouping models

A feasible approach to quantify multipartite nonlocality is to use the *g*-grouping models [9]. Let us consider a model consisting of five parties, i.e., *a*, *b*, *c*, *d*, and *e*. These parties may share some kind of nonlocal communication with each other. Based upon their communication pattern, we can always divide the model into *g* groups such that only parties in the same group are free to communicate with each other. For instance, suppose all the parties are allowed to communicate with each other. Then it can be labeled as $\{abcde\}$ with a grouping number $g = 1$. We will call the model a 1-grouping model. Suppose *a*, *b*, *c*, and *d* can communicate with each other, and *e* cannot. Then the model can be labeled as $\{abcd|e\}$ with a grouping number $g = 2$. We will call the model a 2-grouping model. It needs mention that $\{abc|de\}$ and $\{a|bcde\}$ are also 2-grouping models. Similarly, $\{ab|c|de\}$, $\{a|bcd|e\}$, and $\{ab|cd|e\}$ are 3-grouping models, $\{ab|c|d|e\}$ and $\{a|bc|d|e\}$ are 4-grouping models, and $\{a|b|c|d|e\}$ is a 5-grouping model. It is clear that a model with a smaller

FIG. 1. Illustration of multipartite nonlocality in five-site models. Only sites in the same group (pink shadow) share nonlocal correlations with each other. The leftmost figure illustrates a model with genuine multipartite nonlocality. The rightmost figure illustrates a model without any form of multipartite nonlocality. From left to right, the *hierarchy* of multipartite nonlocality decreases gradually. For general quantum states, the hierarchy of nonlocality can be investigated by Bell-type inequalities.

grouping number *g* contains a higher *hierarchy* of multipartite nonlocality (Fig. 1).

In order to characterize the multipartite nonlocality in a quantum system, we shall try to reproduce its correlations with these grouping models. First, we design some *expression* $\mathcal{S}$ and figure out its maximal value (or the *upper bound*) permitted by *all* the grouping models with a fixed grouping number *g*, i.e., $\mathcal{S} \leqslant \mathcal{S}_g$. Then, for the concerned system, let us evaluate this expression. If the value of $\mathcal{S}$ is within the upper bound, we say that its multipartite nonlocality can be reproduced by *g*-grouping models. Nevertheless, if the value of $\mathcal{S}$ turns out to be beyond the upper bound $\mathcal{S}_g$, we conclude that its multipartite nonlocality cannot be reproduced by any *g*-grouping model. Thus its grouping number is (at most) $g - 1$. In other words, some higher hierarchy of multipartite nonlocality is observed.

For an *n*-qubit quantum state described by a density matrix $\hat{\rho}_n$, a widely used expression to characterize multipartite nonlocality is the expectation value of the Mermin-Klyshko operator, and the corresponding upper bounds are given by the corresponding Bell-type inequalities.

B. Mermin-Klyshko operators and Bell-type inequalities

The *n*-qubit Mermin-Klyshko operator is defined as follows. First, on each qubit *k*, we define two local operators as $\hat{m}_k = \boldsymbol{a}_k \cdot \boldsymbol{\sigma}$ and $\hat{m}'_k = \boldsymbol{b}_k \cdot \boldsymbol{\sigma}$, where $\boldsymbol{a}_k$ and $\boldsymbol{b}_k$ are unit vectors, and elements of $\boldsymbol{\sigma}$ are standard Pauli matrices.

Letting $\hat{M}_1 = \hat{m}_1$ and $\hat{M}'_1 = \hat{m}'_1$, we can construct the *n*-qubit Mermin-Klyshko operator $\hat{M}_n$ recursively as [47,48]

$$\hat{M}_n = \tfrac{1}{2}\hat{M}_{n-1} \otimes (\hat{m}_n + \hat{m}'_n)$$
$$+ \tfrac{1}{2}\hat{M}'_{n-1} \otimes (\hat{m}_n - \hat{m}'_n), \tag{1}$$

where the operator $\hat{M}'_{n-1}$ is obtained by exchanging all the $\boldsymbol{a}_k$ and $\boldsymbol{b}_k$ in $\hat{M}_{n-1}$. It is clear that $\hat{M}_n$ is an *n*-qubit operator depending upon $2n$ unit vectors.

For a quantum state $\hat{\rho}_n$ whose quantum correlations can be reproduced by *g*-grouping models, the following Bell-type inequalities should hold [8–10,16]:

$$\mathcal{S} = \max_{\{\dots \boldsymbol{a}_k, \boldsymbol{b}_k \dots\}} \mathrm{Tr}(\hat{M}_n \hat{\rho}_n) \leqslant 2^{\frac{n-g}{2}} \quad \text{for } n - g \text{ even}, \tag{2}$$

$$\mathcal{S} = \max_{\{\dots \boldsymbol{a}_k, \boldsymbol{b}_k \dots\}} \mathrm{Tr}(\hat{S}_n \hat{\rho}_n) \leqslant 2^{\frac{n-g}{2}} \quad \text{for } n - g \text{ odd}, \tag{3}$$

with $\hat{S}_n = \frac{1}{\sqrt{2}}(\hat{M}_n + \hat{M}'_n)$. The optimization with respect to the unit vectors $\{\dots \boldsymbol{a}_k, \boldsymbol{b}_k \dots\}$ is used to remove any

dependence upon local measures. We mention that these inequalities (combined with the optimized unit vectors) provide feasible measurement settings to carry out Bell-type experiments [49].

When the g-labeled Bell-type inequality is violated, we can conclude that the quantum correlations in the concerned quantum state $\hat{\rho}_n$ cannot be reproduced by any g-grouping model. In other words, the grouping number for the state is (at most) $g - 1$. For instance, the lowest-rank inequality is $\mathcal{S}(\hat{\rho}_n) \leqslant 2^{\frac{n-n}{2}} = 1$ (i.e., $g = n$). If it is violated, we say that the grouping number is (at most) $n - 1$. Thus the lowest hierarchy of nonlocality is observed. On the other hand, the highest-rank inequality is $\mathcal{S}(\hat{\rho}_n) \leqslant 2^{\frac{n-2}{2}}$ (i.e., $g = 2$). If this inequality is violated, the grouping number of $\hat{\rho}_n$ is just 1. In other words, the state presents the highest hierarchy of multipartite nonlocality, i.e., genuine multipartite nonlocality.

It needs mention that the violation of a Bell-type inequality is just a sufficient condition but not a necessary condition for the existence of quantum correlations in the state. For instance, in some specific states, the inequality $\mathcal{S} \leqslant 1$ (the lowest rank one in the whole family) is not violated. Nevertheless, the state may violate some Bell-type inequality from other families [50], and thus its quantum correlations may be observed in other Bell-type experiments. Thereby, the nonviolation of the inequality $\mathcal{S} \leqslant 1$ does not mean quantum correlation is absent in the state. Instead, it just means that no quantum nonlocality would be observed by the current Bell-type experiment.

Although the inequalities in Eqs. (2) and (3) may not be the optimal inequalities for the above-mentioned states, they offer explicit upper bounds for a full family of multipartite correlations (Fig. 1). Therefore, they can disclose nontrivial information about multipartite correlations for general quantum systems, such as the low-dimensional quantum lattices considered in this paper. Moreover, we are just interested in the qualitative behavior of multipartite nonlocality in quantum lattices. Thereby, the parity of $n - g$ would be ignored and we will just consider Eq. (2).

III. MODEL AND SOLUTION

We will investigate an infinite-size bond-alternating spin-$\frac{1}{2}$ Heisenberg chain with next-nearest-neighbor interactions. The model can be described by [42,43]

$$\hat{H} = J_1 \sum_{odd\ i} \mathbf{S}_i \cdot \mathbf{S}_{i+1} + J_2 \sum_{even\ i} \mathbf{S}_i \cdot \mathbf{S}_{i+1} + \alpha \sum_i \mathbf{S}_i \cdot \mathbf{S}_{i+2}.$$

$$(4)$$

The structure of the model is illustrated in Fig. 2. $J_1 = 1 - \delta$ and $J_2 = 1 + \delta$ denote dimerized nearest-neighbor coupling, with $-1 \leqslant \delta \leqslant 1$ the dimerization parameter. $\alpha \geqslant 0$ denotes next-nearest-neighbor coupling.

When $\alpha = 0$, the model would be reduced to a bond-alternating Heisenberg chain with a single parameter δ [42]. In the specific situations $\delta = -1$ and $\delta = 1$, this Heisenberg chain would be further reduced into isolated dimers locating on the odd bonds (i.e., J_1 bonds) and the even bonds (i.e., J_2 bonds), respectively. In fact, the system would be in an odd-Haldane phase for $\delta < 0$ and an even-Haldane
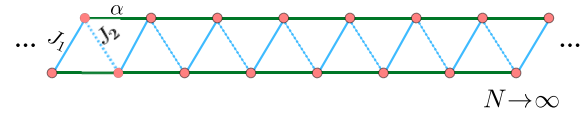

FIG. 2. Structure of an infinite-size bond-alternating spin-$\frac{1}{2}$ Heisenberg chain with next-nearest-neighbor interactions. $J_1 = 1 - \delta \geqslant 0$ and $J_2 = 1 + \delta \geqslant 0$ denote bond-alternating nearest-neighbor coupling, and $\alpha \geqslant 0$ denotes next-nearest-neighbor coupling. For a finite fixed α, when δ increases from -1 to 1, a topological quantum phase transition occurs at $\delta_c = 0$.

phase for $\delta > 0$. When δ increases from -1 to 1, the ground state would undergo a continuous (second-order) QPT at $\delta_c = 0$. Moreover, the nonlocal string-order parameter $\lim_{|i-j| \to \infty} \langle S_{2i} e^{i\pi \sum_{k=2i+1}^{2j-2} S_k} S_{2j-1} \rangle$ changes from a finite value to zero at $\delta_c = 0$ [42]. It reveals that this QPT is accompanied by a change of topological order in the ground state. Thus it is indeed a topological QPT [42].

For a nonzero α, when α is small enough (i.e., $0 < \alpha \leqslant 0.2411$), the nature of the QPT does not change. Explicitly, the ground state still presents a continuous topological QPT at $\delta_c = 0$. When α is larger than 0.2411, nevertheless, the QPT becomes a discontinuous (first-order) topological QPT [51].

In this paper, we will try to characterize these topological QPTs with multipartite nonlocality by considering the reduced density matrices of continuous n-site subchains in the infinite-size model. Both zero temperature and finite temperatures will be studied. For zero temperature, we will use infinite-size matrix product states to approximately describe the ground states. We use the MATRIX PRODUCT TOOLKIT [52] to do the job and the maximum bond dimension is set as $\chi \sim 100$-120. The unit cell of the wave functions consists of four sites, and the SU(2) symmetry is considered so as to improve the accuracy of the wave functions. For finite temperatures, we will use the infinite-size matrix-product-state purification to approximately describe the thermal-state density matrix $\hat{\rho}_T = e^{-\beta \hat{H}}$, with $\beta = \frac{1}{T}$ the inverse temperature [53]. The time slice is set as $\Delta \tau = 0.05$, and we use a second-order Trotter-Suzuki decomposition to reduce the error in decomposing the imaginary-time-evolution operator $e^{-\Delta \tau \hat{H}}$. The maximum bond dimension is set as $\chi = 60$.

The calculation of the nonlocality measure $\mathcal{S}(\hat{\rho}_n)$ is also quite nontrivial since multivariable optimizations are involved in the Bell-type inequalities. In order to deal with large n, one may transform the n-site optimization $\max_{\{\dots \mathbf{a}_k, \mathbf{b}_k \dots\}} \mathrm{Tr}(\hat{M}_n \hat{\rho}_n)$ into a series of two-site optimizations, i.e., $\max_{\{\mathbf{a}_1, \mathbf{b}_1, \mathbf{a}_2, \mathbf{b}_2\}} \mathrm{Tr}(\hat{M}_n \hat{\rho}_n)$, $\max_{\{\mathbf{a}_2, \mathbf{b}_2, \mathbf{a}_3, \mathbf{b}_3\}} \mathrm{Tr}(\hat{M}_n \hat{\rho}_n)$, $\max_{\{\mathbf{a}_3, \mathbf{b}_3, \mathbf{a}_4, \mathbf{b}_4\}} \mathrm{Tr}(\hat{M}_n \hat{\rho}_n)$, and so on. Then we sweep the entire lattice several times until some convergence is obtained. More technical details can be found in Ref. [24]. In our calculations, for each set of physical parameters $\{\delta, \alpha, n, T\}$, 20 independent initial points have been used to carry out the optimizations. Thereby, the optimization results are reliable.

IV. MAIN RESULTS FOR $T = 0$

Before reporting our main results, we mention that there will be two typical ways to select the concerned subchains, i.e., the "odd-bond subchains" in Fig. 3(a) and the "even-bond subchains" in Fig. 3(b). The corresponding reduced density
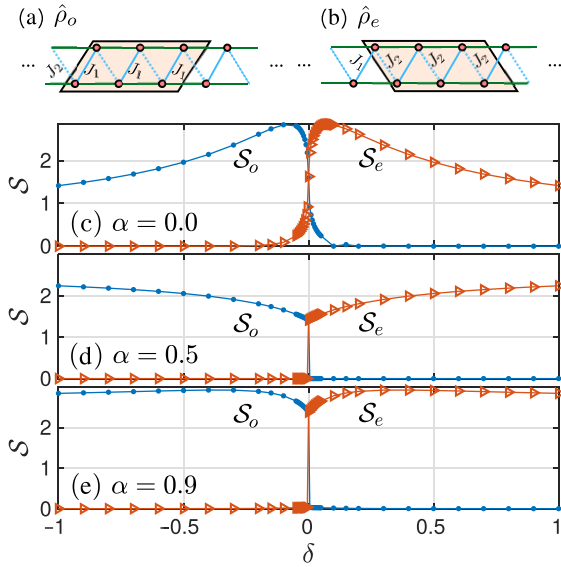
FIG. 3. (a), (b) Two concerned subchains for calculating the nonlocality measures, where the reduced states are denoted by $\hat{\rho}_o$ and $\hat{\rho}_e$, respectively. Since $J_1 = 1 - \delta$ and $J_2 = 1 + \delta$, we have $\hat{\rho}_o(\delta) = \hat{\rho}_e(-\delta)$. (c)–(e) The nonlocality measures as a function of the dimerization parameter δ (with $n = 10$ and $T = 0$). $\mathcal{S}_o$ (dots) corresponds to the odd-bond subchain in (a), and $\mathcal{S}_e$ (triangles) corresponds to the even-bond subchain in (b). For any given δ, we find $\mathcal{S}_o(\delta) = \mathcal{S}_e(-\delta)$.

matrices will be denoted by $\hat{\rho}_o$ and $\hat{\rho}_e$, respectively. Considering $J_1 = 1 - \delta$ and $J_2 = 1 + \delta$, one sees that $\hat{\rho}_o$ and $\hat{\rho}_e$ can be mapped into each other by changing the sign of δ, that is, $\hat{\rho}_o(\delta) = \hat{\rho}_e(-\delta)$. Consequently, the multipartite nonlocality measures for the two subchains can also be mapped to each other by

$$\mathcal{S}_o(\delta) = \mathcal{S}_e(-\delta). \quad (5)$$

To confirm this property, in Figs. 3(c)–3(e), we have illustrated the curves for $\mathcal{S}_o(\delta)$ and $\mathcal{S}_e(\delta)$, which are calculated from completely independent calculations. It is clear that Eq. (5) indeed holds. Thereby, let us first consider odd-bond subchains and use $\mathcal{S}_o$ to begin our investigations.

In Fig. 4, we have shown the multipartite nonlocality measure $\mathcal{S}_o$ as a function of the dimerization parameter δ for various next-nearest-neighbor coupling parameter α. For the first glance, one can see that the $\mathcal{S}_o(\delta)$ curve presents some kind of singularity at the QPT point $\delta_c = 0$. For $\alpha = \{0, 0.2\}$, $\mathcal{S}_o$ is continuous and its derivative $\frac{d\mathcal{S}_o}{d\delta}$ diverges at $\delta_c = 0$, and thus signals the second-order QPTs. For $\alpha = \{0.4, 0.5, 0.7, 0.9\}$, $\mathcal{S}_o$ is discontinuous at $\delta_c = 0$, and thus signals the first-order QPTs.

Second, we pay attention to the n dependence of $\mathcal{S}_o$. In the even-Haldane phase $\delta > \delta_c$, except for narrow regions near the QPT point $\delta = \delta_c$, the value of the nonlocality measure is

$$\mathcal{S}_o = 0. \quad (6)$$

In fact, when the length of the subchains increases from $n = 10$ to $n = 20$, we have not observed considerable growth of $\mathcal{S}_o$.

In the odd-Haldane phase $\delta < \delta_c$, nevertheless, $\mathcal{S}_o$ is relatively large. One can see that as n increases from 10 to 20, $\mathcal{S}_o$
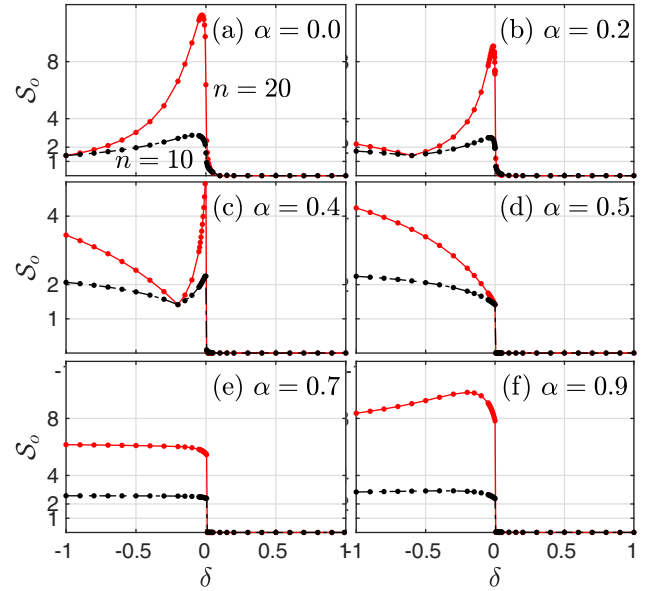

FIG. 4. Multipartite nonlocality measure $\mathcal{S}_o$ as a function of the dimerization parameter δ for various next-nearest-neighbor coupling parameter α, with $n = 10$ (black dashed curves) and $n = 20$ (red solid curves). The horizontal grid lines represent the threshold of the Bell-type inequalities $\mathcal{S} \leqslant 1, 2, 4, 8$ in Eq. (2). $\delta_c = 0$ is the quantum phase transition point.

increases significantly for most δ. We have further calculated the nonlocality measure $\mathcal{S}_o$ with n up to 50, and the scaling behavior for several coupling constants is shown in Fig. 5. One can see that when n is large enough, the logarithm nonlocality measure presents a linear dependence upon n, i.e.,

$$\log_2 \mathcal{S}_o \sim \mathcal{K}n + b, \quad (7)$$

with $\mathcal{K}$ and b two fitting parameters.

Moreover, at several special points, the nonlocality measure $\mathcal{S}_o$ is size independent. That is, at $\delta^* = -1$ in Fig. 4(a), $\delta^* = -0.6$ in Fig. 4(b), $\delta^* = -0.2$ in Fig. 4(c), and $\delta^* = 0$ in Fig. 4(d), we always find
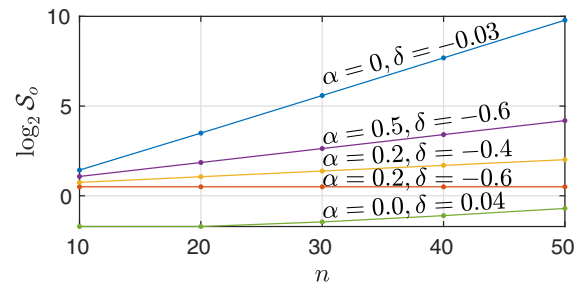
$$\mathcal{S}_o = 1.414, \quad (8)$$

FIG. 5. The n dependence of the nonlocality measure $\mathcal{S}_o$ at zero temperature with various coupling constants. When n is large enough, we have $\log_2 \mathcal{S}_o \sim \mathcal{K}n + b$. This behavior holds in the entire odd-Haldane phase and in a rather narrow region $\delta \approx \delta_c^+$ of the even-Haldane phase (in most regions of this phase, we simply have $\mathcal{S}_o = 0$).
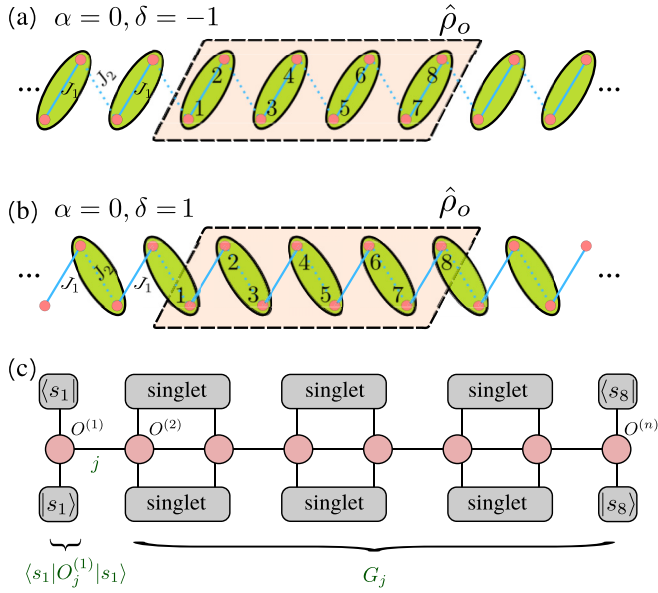
FIG. 6. Two special situations with (a) $\alpha = 0, \delta = -1$ and (b) $\alpha = 0, \delta = 1$. In (a), $\hat{\rho}_o$ is a pure state, for which the nonlocality measure is $\mathcal{S}_o = \sqrt{2}$. In (b), $\hat{\rho}_o$ is a mixed state, for which the nonlocality measure turns out to be $\mathcal{S}_o = 0$ exactly. (c) A tensor network for $f_{s_1 s_8}$, which is used to explain why $\mathcal{S}_o = 0$ for the situation given in (b).

for any finite n. It needs mention that $\mathcal{S} = \sqrt{2}$ is a typical value for the singlet state $|\psi_{i,i+1}\rangle = \frac{1}{\sqrt{2}}(|\uparrow\downarrow\rangle - |\downarrow\uparrow\rangle)$ [54]. A size-independent value of $\mathcal{S}_o = 1.414$ strongly suggests that the ground states of the chains are just the product of these singlets, i.e., $|\Psi\rangle = \bigotimes_{i=1,3,5...} |\psi_{i,i+1}\rangle$. Please see Fig. 6(a). Further analysis shows that all these size-independent points locate on the line $-2\alpha + \delta = -1$. Thus, our result confirms the conjecture that on this line, the ground states are decoupled into singlets [43,55]. Moreover, since the quantum state $|\Psi\rangle$ just contains local two-site correlations (rather than other nontrivial multipartite correlations), the measure $\mathcal{S}_o$ is rather small. That is why $\mathcal{S}_o$ presents a minimum at $\delta = \delta^*$ in the $\mathcal{S}_o(\delta)$ curves in Fig. 4.

Third, we characterize the odd-Haldane phase in $\delta < \delta_c$ with Bell-type inequalities and multipartite nonlocality. According to Fig. 4, it is quite clear that some Bell-type inequalities are violated. Moreover, as n increases, $\mathcal{S}_o$ increases steadily for most $\delta < \delta_c$. Thus, in the large-n limit, it is expected that rather high-rank Bell-type inequalities would be violated. Consequently, high-hierarchy nonlocality would be observed in the odd-bond subchains.

A detailed analysis about the grouping number g may be interesting. We mention that for $g = n, n - 2, n - 4, n - 6, \dots$, the upper bounds of the nonlocality measure permitted by g-grouping models are given by the Bell inequalities $\mathcal{S} \leqslant 1, 2, 4, 8, \dots$, respectively. In Fig. 4, we have used some horizontal grid lines to represent these upper bounds. Let us just pay attention to $\{\alpha = 0, n = 20\}$ in Fig. 4(a), and other curves in the figure can be analyzed in a straightforward way. For $\delta \lesssim -0.73$, one sees that the lowest-rank inequality $\mathcal{S} \leqslant 1$ is violated. It means that the correlations cannot be reproduced by $(g = n)$-grouping models. In other words, the grouping number is (at most) $g = n - 1$. As δ increases, in the range

$-0.73 \lesssim \delta \lesssim -0.38$, the inequality $\mathcal{S} \leqslant 2$ is further violated. Thus the corresponding grouping number is (at most) $g = n - 3$.

Then, for $-0.38 \lesssim \delta \lesssim -0.14$, the inequality $\mathcal{S} \leqslant 4$ is also violated. Thus the grouping number is reduced to be (at most) $g = n - 5$.

In the range $-0.14 \lesssim \delta \lesssim -0.002$, the inequality $\mathcal{S} \leqslant 8$ is violated and the grouping number becomes (at most) $g = n - 7$.

In the vicinity of the critical point $\delta_c = 0$, the nonlocality measure decreases sharply. It indicates that multipartite correlations in the ground states change dramatically in the QPT.

Fourth, we shall turn our attention to multipartite correlations in the even-Haldane phase in $\delta > \delta_c$.

In most regions in this phase, we numerically find $\mathcal{S}_o = 0$. To understand these unexpected numerical results, let us consider an exactly soluble point $\{\alpha = 0, \delta = 1\}$. At this point, all the α bonds and J_1 bonds in the lattice would be broken, and thus the ground state would be a product state of the singlets $|\psi_{i,i+1}\rangle$ on the J_2 bonds (or even bonds). Please see Fig. 6(b).

Consequently, the concerned odd-bond subchain (we take $n = 8$, for instance) would be in a mixed state. It is easy to prove that this mixed state is given by $\hat{\rho}_o = \frac{1}{4} \sum_{s_1 s_8} |\Psi_{s_1 s_8}\rangle\langle\Psi_{s_1 s_8}|$, where $|\Psi_{s_1 s_8}\rangle = |s_1\rangle \otimes |\psi_{2,3}\rangle \otimes |\psi_{4,5}\rangle \otimes |\psi_{6,7}\rangle \otimes |s_8\rangle$ with $s_{1,8} = \{\uparrow, \downarrow\}$. Thereby, the objective function $\text{Tr}(\hat{M}_n \hat{\rho}_n)$ on the left-hand side of the Bell inequalities should be expressed as $\text{Tr}(\hat{M}_n \hat{\rho}_o) = \frac{1}{4}(f_{\uparrow\uparrow} + f_{\downarrow\uparrow} + f_{\uparrow\downarrow} + f_{\downarrow\downarrow})$, with $f_{s_1 s_8} = \langle\Psi_{s_1 s_8}|\hat{M}_n(\dots \boldsymbol{a}_k, \boldsymbol{b}_k \dots)|\Psi_{s_1 s_8}\rangle$. For each $f_{s_1 s_8}$, we find that the optimal value is just $\sqrt{2}$, but $f_{\uparrow\uparrow}, f_{\downarrow\uparrow}, f_{\uparrow\downarrow}$, and $f_{\downarrow\downarrow}$ cannot achieve $\sqrt{2}$ simultaneously. Instead, for arbitrary unit vectors $\{\dots \boldsymbol{a}_k, \boldsymbol{b}_k \dots\}$, we can prove that $f_{\uparrow\uparrow} = -f_{\downarrow\uparrow}$ and $f_{\uparrow\downarrow} = -f_{\downarrow\downarrow}$,[1] and thus we always have $\text{Tr}(\hat{M}_n \hat{\rho}_o) = 0$. Consequently, for the state $\hat{\rho}_o$ in Fig. 6(b), we have $\mathcal{S}_o = \max_{\{\dots \boldsymbol{a}_k, \boldsymbol{b}_k \dots\}} \text{Tr}(\hat{M}_n \hat{\rho}_o) = 0$.

We have figured out an analytic result $\mathcal{S}_o = 0$ for the exactly soluble point $\{\alpha = 0, \delta = 1\}$. It is believed that the numerical results $\mathcal{S}_o = 0$, which are widely observed in the even-Haldane phase in Fig. 4, can also be explained by a similar process.

We mention that $\mathcal{S}_o = 0$ does not mean that quantum correlation completely vanishes in the even-Haldane phase. For instance, in Fig. 6(b), quantum correlations still exist in the singlets $|\psi_{2,3}\rangle, |\psi_{4,5}\rangle$, and $|\psi_{6,7}\rangle$. The violation of some Bell-type inequality is just a sufficient condition but not a necessary condition for the existence of quantum correlations in the systems. Thereby, the nonviolation of a Bell-type inequality (since $\mathcal{S}_o = 0$) just indicates that no quantum nonlocality could be observed by the current Bell-type inequalities and experiments. Let us resort to the relation $\mathcal{S}_o(\delta) = \mathcal{S}_e(-\delta)$. Then the large values of $\mathcal{S}_o$ in the regions $\delta < 0$ in Fig. 4

---

[1] In Fig. 6(c), we have illustrated a tensor network for $f_{s_1 s_8}$, where $|\Psi_{s_1 s_8}\rangle$ and $\hat{M}_8$ are expressed as a matrix product state and a matrix product operator, respectively. Based on this network, $f_{s_1 s_8}$ can be rephrased as $\sum_j \langle s_1|O_j^{(1)}|s_1\rangle G_j$. Then it is straightforward that $f_{\uparrow s_8} + f_{\downarrow s_8} = \sum_j \text{Tr}(O_j^{(1)}) G_j$. Note that $O_1^{(1)} = \hat{m}_k = \boldsymbol{a}_k \cdot \boldsymbol{\sigma}$ and $O_2^{(1)} = \hat{m}'_k = \boldsymbol{b}_k \cdot \boldsymbol{\sigma}$, both of which are zero-trace operators [45]. Therefore, we shall always have $f_{\uparrow s_8} + f_{\downarrow s_8} = 0$.

immediately indicate that $\mathcal{S}_e$ would present large values in $\delta > 0$. In other words, when we carry out Bell-type experiments on the even-bond subchains [Fig. 3(b)], high-hierarchy multipartite nonlocality would be observed in this phase.

We are ready to figure out a conclusion about multipartite nonlocality and QPTs in the model. Both the even-Haldane phase and the odd-Haldane phase present nontrivial multipartite nonlocality. Nevertheless, in the two phases, the spread (or existence form) of multipartite nonlocality among the lattice is different. When Bell-type experiments are carried out on odd-bond subchains, the high hierarchy of multipartite nonlocality can be observed in the odd-Haldane phase but not in the even-Haldane phase. When even-bond chains are considered, the result is reversed. In both situations, the nonlocality measure $\mathcal{S}_o$ (and $\mathcal{S}_e$) would be large in one phase and vanish in the other phase, and offers quite sharp signals for the QPTs.

Finally, we discuss the influence of the next-nearest-neighbor coupling α upon the multipartite nonlocality in the model. As we have mentioned, α drastically shapes the singularity of the $\mathcal{S}_o(\delta)$ curves at $\delta = \delta_c$ (Fig. 4). That is, $\frac{\partial \mathcal{S}_o}{\partial \delta}$ is divergent for small α, and $\mathcal{S}_o$ itself is discontinuous for large α. Our other concern is that for a fixed value of δ, would α have a concise influence upon the value of the nonlocality measure? Since $\mathcal{S}_o(\delta) = \mathcal{S}_e(-\delta)$, we shall just pay attention to $\mathcal{S}_o$. We will study two typical situations, i.e., $\delta = -1$ and $\delta = \delta_c$. First, we consider the situation $\delta = -1$, where the model would be reduced into a ladder, with $J_1 = 2$ the in-rung coupling (the blue solid bonds in Fig. 2) and α the in-leg coupling (the green bonds in Fig. 2). From the result with $n = 20$ in Fig. 4, we find that when α is equal to 0, 0.2, 0.4, 0.5, 0.7, and 0.9, the value of $\mathcal{S}_o|_{\delta=-1}$ is equal to 1.414, 2.222, 3.446, 4.239, 6.158, and 8.364, respectively. Thus a *monotonic increasing* behavior is observed. The physical picture is quite clear. When $\alpha = 0$, the model is reduced into isolated dimers, which merely have $\mathcal{S}_o = 1.414$. As α increases, these dimers would be combined into a ladder, and then multipartite nonlocality can spread along the two legs. That is why α tends to enhance multipartite nonlocality. Nevertheless, when we consider the situations $\delta \neq -1$, the result becomes rather complex. In Fig. 2, one can see that the three antiferromagnetic bonds (labeled $J_1 = 1 - \delta$, $J_2 = 1 + \delta$, and α) form a triangle, and thus quantum frustration [56] emerges. Consequently, a classical physical picture no longer exists. In fact, for the situation $\delta = -0.005 \approx \delta_c$, when α is equal to 0, 0.2, 0.4, 0.5, 0.7, and 0.9, the value of $\mathcal{S}_o$ is equal to 9.758, 8.698, 4.947, 1.453, 5.571, and 8.033, respectively. Thus, $\mathcal{S}_o$ is *not a monotonic function* of α any more. Thereby, the influence of the next-nearest-neighbor coupling α upon multipartite nonlocality is quite model dependent, and we cannot always figure out a compact conclusion.

V. MAIN RESULTS FOR FINITE TEMPERATURES

In this section, we report our results of finite-temperature nonlocality in the model. We pay attention to the influence of the temperature upon both the $\mathcal{S}(\delta)$ curves and the scaling curves $\log_2 \mathcal{S}(n)$. The model with $\alpha = 0.2$ will be used as an example for the second-order QPTs and $\alpha = 0.4$ for the first-order QPTs. Moreover, considering the relation $\mathcal{S}_o(\delta) = \mathcal{S}_e(-\delta)$, we will just consider the nonlocality measure $\mathcal{S}_o$.
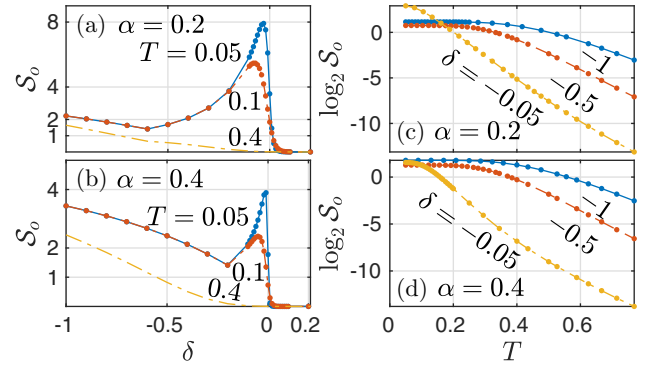

FIG. 7. Multipartite nonlocality measure $\mathcal{S}_o$ at finite temperatures. (a),(b) The influence of the temperature T upon the $\mathcal{S}_o(\delta)$ curves. The horizontal grid lines represent the threshold of the Bell-type inequalities $\mathcal{S} \leqslant 1, 2, 4, \ldots$ in Eq. (2). (c), (d) The logarithm nonlocality measure as a function of the temperature for various coupling constants. The length of the subchain is $n = 20$.

A. $\mathcal{S}_o(\delta)$ curves at finite temperatures

In Fig. 7, we have illustrated the $\mathcal{S}_o(\delta)$ curves with several temperatures for (a) $\alpha = 0.2$ and (b) $\alpha = 0.4$. Let us first consider low temperatures, i.e., $T = 0.05$ and $T = 0.1$. One can see that in noncritical regions, the $\mathcal{S}_o(\delta)$ curves are quite consistent with the corresponding zero-temperature curves in Fig. 4. The mechanics is that there is a finite energy gap above the ground-state energy level, which prevents low-energy excited states from contributing to the thermal state $\hat{\rho}_T = e^{-\beta \hat{H}}$ (and, consequently, $\mathcal{S}_o$) at low temperatures. In the critical regions $\delta \approx \delta_c$, on the other hand, as T rises from 0.05 to 0.1, the peak of the $\mathcal{S}_o(\delta)$ curve presents a considerable decline. The underlying mechanics is that the system is gapless at the critical point $\delta = \delta_c$, and thus $\hat{\rho}_T$ (and, consequently, $\mathcal{S}_o$) is significantly affected by low-lying excited states. Finally, as can be seen in Fig. 7, the footprints of the QPTs would survive when the temperature is low enough.

We then consider a relatively high temperature $T = 0.4$. One can see that the peak completely disappears in the $\mathcal{S}_o(\delta)$ curve for $T = 0.4$. This is because, when the temperature is high enough, too many high-lying excited states incoherently mix into the thermal state $\hat{\rho}_T$, and thus destroy the quantum correlations.

In order to offer a quantitative description about the effect of the temperature, we have illustrated the logarithm measure $\log_2 \mathcal{S}_o$ as a function of T in Fig. 7(c) for $\alpha = 0.2$ and in Fig. 7(d) for $\alpha = 0.4$. In the low-temperature regions, $\log_2 \mathcal{S}_o$ is *robust* against thermodynamic fluctuations in noncritical regions ($\delta = -0.5$ and $\delta = -1$), and is relatively *sensitive* to thermodynamic fluctuations in the critical regions ($\delta = -0.05$). These results are consistent with Figs. 7(a) and 7(b).

B. Scaling at finite temperatures

We then turn our attention to the scaling behavior of the finite-temperature nonlocality measure. We will just take the situation with $\{\alpha = 0, \delta = -0.03\}$, for instance, where the model is in the vicinity of the critical point $\delta_c = 0$. Our results for several temperatures can be found in Fig. 8(a).
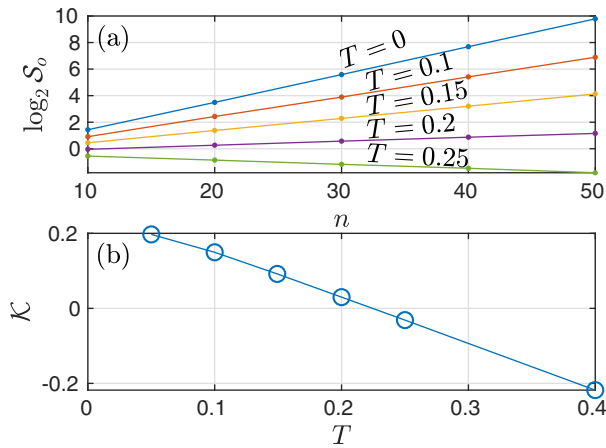
FIG. 8. (a) The n dependence of the nonlocality measure $\mathcal{S}_o$ at finite temperatures with $\{\alpha = 0, \delta = -0.03\}$. The scaling behavior $\log_2 \mathcal{S}_o \sim \mathcal{K}n + b$ survives at finite temperatures. (b) As the temperature rises, the slope $\mathcal{K}$ presents an approximately linear decline.

It is clear that at finite temperatures, the linear scaling formula still holds, i.e.,

$$\log_2 \mathcal{S}_o \sim \mathcal{K}n + b, \qquad (9)$$

where b is a quite small number and can be omitted in the large-n limit.

Since the scaling formula holds both for zero temperature and finite temperatures, it may be helpful to explain the physical meaning of the quantity $\mathcal{K}$ before we continue our discussions. Our point is that while the nonlocality measure $\mathcal{S}$ characterizes multipartite nonlocality in general *finite*-size systems, the parameter $\mathcal{K}$ can characterize multipartite nonlocality in the large-n limit.

It is well known that the upper bound of the Bell-type inequalities permitted by quantum mechanism is $\mathcal{S} = 2^{\frac{n-1}{2}}$, in other words,

$$\log_2 \mathcal{S} = \tfrac{1}{2}n - \tfrac{1}{2}. \qquad (10)$$

Thereby, it is clear that for general quantum chains, we should have $\mathcal{K} \leqslant \frac{1}{2}$.

For a system, suppose it turns out that $\mathcal{K} = \frac{1}{2}$ and thus $\mathcal{S} \sim 2^{\frac{1}{2}n+b}$. It is clear that some highest-rank Bell-type inequalities (such as $\mathcal{S} \leqslant 2^{\frac{n-2}{2}}$ and $\mathcal{S} \leqslant 2^{\frac{n-3}{2}}$) would be violated. Moreover, the grouping number g would be a quite small number (such as 2 and 3, determined by b). Thereby, the system contains a high hierarchy of multipartite nonlocality. Suppose the physical parameters (i.e., magnetic field or temperature) of the system change and thus $\mathcal{K}$ is reduced to $\frac{1}{3}$ and we have $\mathcal{S} \sim 2^{\frac{1}{3}n+b}$. Then the Bell-type inequality $\mathcal{S} \leqslant 2^{\frac{n-g}{2}}$ with $g \approx \frac{n}{3}$ would be violated. It means that the upper bound of the grouping number is about $\frac{n}{3}$, and thus a relatively low hierarchy of multipartite nonlocality would be observed with the current Bell-type experiment. Suppose $\mathcal{K}$ is further reduced to $\frac{1}{4}$. Then it is straightforward that the upper bound of the grouping number would become as large as $g \approx \frac{n}{2}$, and thus the hierarchy of nonlocality observed in the current Bell-type experiment is even lower. Suppose $\mathcal{K}$ turns out to be 0 and thus $\mathcal{S} \sim 2^b$. Since b is usually quite small, only the lowest-

rank Bell inequalities (such as $\mathcal{S} \leqslant 1$ and $\mathcal{S} \leqslant 2$) may be violated. Thereby, merely the lowest hierarchy of nonlocality can be observed. Finally, suppose $\mathcal{K}$ is reduced to be negative. Then the nonlocality measure $\mathcal{S} \sim 2^{\mathcal{K}n+b}$ would be zero in the large-n limit and no Bell inequality would be violated. In other words, no quantum nonlocality could be observed by current Bell-type experiments.

From the above discussions, we can see that the slope $\mathcal{K} \in (-\infty, \frac{1}{2}]$ offers us a quite valuable and intuitive tool to characterize nonlocality in infinite-size chains. Thereby, it would be interesting to investigate the influence of the temperature upon the slope $\mathcal{K}$ in the model.

In Fig. 8(b), we have illustrated the slope $\mathcal{K}$ as a function of the temperature T for the model with $\{\alpha = 0, \delta = -0.03\}$. As the temperature rises, it is quite interesting that $\mathcal{K}$ presents an approximately linear decline, i.e.,

$$\mathcal{K} \approx -pT + q, \qquad (11)$$

with p and q two fitting parameters. According to the above discussions about the physical meaning of $\mathcal{K}$, this result indicates that in infinite-size chains, as the temperature rises, the hierarchy of multipartite nonlocality observed in the current Bell-type experiment is reduced steadily and linearly.

When quantum correlations are used as a resource to carry out quantum information tasks [57], the threshold temperature T_c below which quantum correlations can be experimentally detected is an important quantity. For the multipartite nonlocality considered in this paper, first, it is quite clear that the threshold condition is $\mathcal{K}(T_c) = 0$, with T_c the threshold temperature. In fact, according to Eq. (9), one can see that in the large-n limit, $\mathcal{S}$ would vanish if $\mathcal{K} < 0$ and tend to infinity if $\mathcal{K} > 0$. Thus, $\mathcal{K}(T_c) = 0$ is indeed the threshold condition. It is quite promising that the linear decline behavior in Eq. (11) can help us to estimate this threshold temperature. We have used Eq. (11) to fit the six data points in Fig. 8(b), and find $p = 1.199$ and $q = 0.266$. Thereby, T_c turns out to be $T_c = \frac{q}{p} = 0.222$. On the other hand, we have also used the two data points at $T = 0.2$ and $T = 0.25$ to figure out p and q, which gives $T_c = 0.224$.

Finally, combined with Eqs. (9) and (11), we shall have

$$\log_2 \mathcal{S}_o \sim -pnT + qn + b. \qquad (12)$$

Thereby, for a finite-size system with a fixed length n, it is expected that as the temperature rises, the logarithm measure would decrease linearly. In fact, as can be seen in Figs. 7(c) and 7(d), when the temperature is not too low, $\log_2 \mathcal{S}_o$ in finite-size subchains indeed presents an approximately linear decline when T rises.

VI. SUMMARY AND DISCUSSIONS

In this paper, we have studied multipartite nonlocality and Bell-type inequalities in bond-alternating spin-$\frac{1}{2}$ Heisenberg chains with next-nearest-neighbor interactions, which undergo topological QPTs at zero temperature.

Our main observation is that multipartite nonlocality can characterize these topological QPTs quite well. Because of the symmetry of the model, the nonlocality measure on odd-bond subchains (i.e., $\mathcal{S}_o$) and the nonlocality measure on even-bond subchains (i.e., $\mathcal{S}_e$) have a relation $\mathcal{S}_o(\delta) = \mathcal{S}_e(-\delta)$, with

$-1 \leqslant \delta \leqslant 1$ the dimerization parameter in the model. When odd-bond subchains are considered, in the odd-Haldane phase in $\delta < 0$, $\mathcal{S}_o$ is large and a high hierarchy of multipartite nonlocality is observed, while in most regions of the even-Haldane phase in $\delta > 0$, the measure $\mathcal{S}_o$ is simply zero. When even-bond subchains are considered, opposite results would be observed. Thereby, high-hierarchy multipartite nonlocality is present in both phases, but the spread of multipartite nonlocality in the lattice is different. Moreover, at the QPT point $\delta = 0$, both $\mathcal{S}_o$ and $\mathcal{S}_e$ present sharp signals for these QPTs. For the second-order QPTs with $\alpha = 0$ and $\alpha = 0.2$, the derivatives of the two measures diverge at $\delta = 0$. For the first-order QPTs with $\alpha = 0.4$, $\alpha = 0.5$, $\alpha = 0.7$, and $\alpha = 0.9$, the two measures themselves are discontinuous at $\delta = 0$. These results reveal that these topological QPTs are accompanied by a dramatic change of multipartite quantum correlations.

The underlying mechanics of why multipartite nonlocality can describe these topological QPTs deserves some discussion. It is well known that when a topological QPT occurs, some nonlocal orders in the entire system change dramatically. Thus, the success of multipartite nonlocality suggests that it has captured some fundamental change of nonlocal correlations in the ground states in the model. To clarify this point, we pay attention to the scaling behavior of the multipartite nonlocality measures, for instance, $\mathcal{S}_o$. For the odd-Haldane phase in $\delta < 0$, as n increases, $\mathcal{S}_o$ increases *exponentially*. Thus, $\mathcal{S}_o$ has successfully captured some nonlocal correlations in the odd-Haldane phase. For the even-Haldane phase in $\delta > 0$, nevertheless, as n increases from 10 to 20, $\mathcal{S}_o$ *remains zero* in most of the regions (Fig. 4). Thus, $\mathcal{S}_o$ has not captured any nonlocal correlation in the even-Haldane phase. This sharp difference reveals unambiguously that the nonlocal correlations in the two phases are different. The fundamental mechanics for multipartite nonlocality to successfully characterize these topological QPTs is that (1) multipartite nonlocality naturally captures nonlocal correlations, while (2) one of the features of topological QPTs is the change of nonlocal orders in the systems.

Moreover, we have also considered the influence of the next-nearest-neighbor coupling (described by α) upon the multipartite nonlocality in the model. In the situation $\delta = -1$, we find that α tends to enhance multipartite nonlocality in the model. For other regions such as $\delta = -0.005$, nevertheless, the measure $\mathcal{S}$ is no longer a monotonic function of α. Thus, the effect of the next-nearest-neighbor coupling turns out to be quite model dependent. We would like to mention that the antiferromagnetic next-nearest-neighbor coupling actually introduces *quantum frustration* into the system. Quantum frustration is an important phenomenon in condensed matter physics and can be quantified by some advanced methods [58,59]. Studying the relationship between multipartite nonlocality and quantum frustration (rather than the coupling parameter α itself) may provide an opportunity to get a more essential physical picture and we will investigate the issue in our future work.

In addition to zero temperature, with the help of thermal-state tensor networks, we have also studied multipartite nonlocality in the model at finite temperatures. First of all, we have found that at low temperatures, the $\mathcal{S}_o(\delta)$ curves

still present some footprints for the topological QPTs. Then we have turned our attention to the large-n behavior of the finite-temperature nonlocality. For the model considered in this paper, we find the scaling formula $\log_2 \mathcal{S}_o \sim \mathcal{K}n + b$ survives at finite temperatures. Based upon this scaling, we argue that the slope $\mathcal{K}$ is a valuable tool to characterize finite-temperature nonlocality in the large-n limit. Explicitly, $\mathcal{K} \to \frac{1}{2}$ indicates the highest hierarchy of nonlocality in the concerned states $\hat{\rho}_{n \to \infty}$, $\mathcal{K} \to 0$ indicates the lowest hierarchy of nonlocality, and $\mathcal{K} < 0$ indicates that no nonlocality would be detected by the current Bell-type inequalities or experiments. Then we have used $\mathcal{K}$ to characterize the influence of the temperature upon multipartite nonlocality in the model and found that $\mathcal{K} \sim -pT + q$, with p and q two fitting parameters. This result indicates that in infinite-size chains, as the temperature rises, the hierarchy of the multipartite nonlocality observed in the current Bell-type experiment would reduce steadily and linearly. This linear decline behavior of $\mathcal{K}$ can be used to estimate the threshold temperature T_c below (above) which multipartite nonlocality can (cannot) be observed by the current Bell-type experiments. We would like to mention that the nonlocality measure $\mathcal{S}$ has been used to characterize several finite-size chains or subchains at finite temperatures [45,60]. This result in the large-n limit is a necessary supplement to previous papers.

It is known that low-dimensional quantum spin models can be experimentally simulated using some advanced techniques, such as trapped ions and ultracold atoms [61–64]. Recently, multipartite nonlocality has also been observed in several well-designed experiments on trapped ions [49] and photons [65,66]. It is quite remarkable that in Ref. [49], the nonlocality measure in $n = 7$ qubits has been estimated experimentally. Therefore, it is technically feasible to design some experiment to realize the main result in this paper. First of all, one may use trapped ions to simulate the spin chain model defined in Eq. (4). Second, in order to estimate the nonlocality measure $\mathcal{S}$ (which is a combination of 2^n expectation values), we need to (i) optimize local measurement settings $\{\dots \boldsymbol{a}_k, \boldsymbol{b}_k \dots\}$ and (ii) experimentally estimate each of the 2^n expectation values [49]. From an experimental point of view, both steps are quite nontrivial. Nevertheless, our theoretical investigations can help simplify the experimental process. For step (i), we mention that our numerical results can explicitly provide a set of optimal measurement settings. For instance, along the line $-2\alpha + \delta = -1$, we numerically find that the optimal angles are translation invariant, i.e., $\boldsymbol{a}_k = \boldsymbol{b}_k = (\frac{\sqrt{2}}{2}, 0, \frac{\sqrt{2}}{2})$ for $1 \leqslant k \leqslant n$. For step (ii), one can see that when n is large, it would be rather inconvenient to measure 2^n observables so as to figure out $\mathcal{S}$. Fortunately, the linear scaling $\log_2 \mathcal{S} \sim \mathcal{K}n + b$ illustrated in Fig. 5 provides a simplified method to estimate $\mathcal{S}$ for large n. Explicitly, we can first figure out $\mathcal{S}$ experimentally with n up to 7 [49], then use these data to fit the parameters $\mathcal{K}$ and b, and finally estimate the value of $\mathcal{S}$ for large n. Thereby, our theoretical investigations on multipartite nonlocality can provide valuable guidance for carrying out corresponding experiments in one-dimensional (1D) quantum chains.

Finally, we mention that in the vicinity of the critical points, as δ changes, the multipartite nonlocality measure $\mathcal{S}_o$ (and $\mathcal{S}_e$) is quite *sensitive* (Fig. 3). In a quite recent paper,

this kind of sensitivity in the multipartite nonlocality has been used in quantum-enhanced metrology [67]. Because of the gaplessness feature at these critical points, the measure $\mathcal{S}_o$ presents some kind of sensitivity even at finite temperatures (Fig. 7). Thereby, multipartite nonlocality at finite temperatures may be used as a resource for quantum-enhanced thermometry [68–73]. According to the scaling formula in Eq. (12), $\mathcal{S}_o$ is an exponential function of the temperature T as $\mathcal{S}_o \sim 2^{-pnT}$, where the exponent n is the number of qubits. One can see that by increasing n, $\mathcal{S}_o$ would become even more sensitive, which means that we may obtain a higher precision in quantum thermometry. This qualitative conclusion that "increasing the number of qubits can improve the sensitivity and the achievable precision" is consistent with the results in [67]. On the other hand, for larger n, because of the 2^n

nonlocal collective measures, the experiment would become more unfeasible [69]. Thereby, there is a fundamental contradiction between the precision and experimental operability, and we can achieve some trade-off by adjusting n. It would be interesting to consider this topic in more depth in our future research.

[1] J. Eisert, M. Cramer, and M. B. Plenio, Rev. Mod. Phys. **82**, 277 (2010).

[2] N. Laflorencie, E. S. Sørensen, M.-S. Chang, and I. Affleck, Phys. Rev. Lett. **96**, 100603 (2006).

[3] D. A. Meyer and N. R. Wallach, J. Math. Phys. **43**, 4273 (2002).

[4] T. R. de Oliveira, G. Rigolin, M. C. de Oliveira, and E. Miranda, Phys. Rev. Lett. **97**, 170401 (2006).

[5] F. Levi and F. Mintert, Phys. Rev. Lett. **110**, 150402 (2013).

[6] G. D. Chiara and A. Sanpera, Rep. Prog. Phys. **81**, 074002 (2018).

[7] V. Scarani and N. Gisin, J. Phys. A: Math. Gen. **34**, 6043 (2001).

[8] D. Collins, N. Gisin, S. Popescu, D. Roberts, and V. Scarani, Phys. Rev. Lett. **88**, 170405 (2002).

[9] J.-D. Bancal, C. Branciard, N. Gisin, and S. Pironio, Phys. Rev. Lett. **103**, 090503 (2009).

[10] J.-D. Bancal, N. Brunner, N. Gisin, and Y.-C. Liang, Phys. Rev. Lett. **106**, 020405 (2011).

[11] N. Brunner, J. Sharam, and T. Vértesi, Phys. Rev. Lett. **108**, 110501 (2012).

[12] J.-D. Bancal, J. Barrett, N. Gisin, and S. Pironio, Phys. Rev. A **88**, 014102 (2013).

[13] J. Batle and M. Casas, Phys. Rev. A **82**, 062101 (2010).

[14] E. G. Cavalcanti, Q. Y. He, M. D. Reid, and H. M. Wiseman, Phys. Rev. A **84**, 032115 (2011).

[15] Q. Y. He, P. D. Drummond, and M. D. Reid, Phys. Rev. A **83**, 032120 (2011).

[16] J. Batle and M. Casas, J. Phys. A: Math. Theor. **44**, 445304 (2011).

[17] R. Chaves, A. Acín, L. Aolita, and D. Cavalcanti, Phys. Rev. A **89**, 042106 (2014).

[18] S. Sami, I. Chakrabarty, and A. Chaturvedi, Phys. Rev. A **96**, 022121 (2017).

[19] Y. Dai, C. Zhang, W. You, Y. Dong, and C. H. Oh, Phys. Rev. A **96**, 012336 (2017).

[20] S. Sachdev, *Quantum Phase Transitions* (Cambridge University Press, Cambridge, 1999).

[21] F. Altintas and R. Eryigit, Ann. Phys. **327**, 3084 (2012).

[22] Z.-Y. Sun, Y.-Y. Wu, J. Xu, H.-L. Huang, B.-F. Zhan, B. Wang, and C.-B. Duan, Phys. Rev. A **89**, 022101 (2014).

[23] Z.-Y. Sun, S. Liu, H.-L. Huang, D. Zhang, Y.-Y. Wu, J. Xu, B.-F. Zhan, H.-G. Cheng, C.-B. Duan, and B. Wang, Phys. Rev. A **90**, 062129 (2014).

[24] Z.-Y. Sun, B. Guo, and H.-L. Huang, Phys. Rev. A **92**, 022120 (2015).

[25] Z.-Y. Sun, X. Guo, and M. Wang, Eur. Phys. J. B **92**, 75 (2019).

[26] H.-G. Cheng, M. Li, Y.-Y. Wu, M. Wang, D. Zhang, J. Bao, B. Guo, and Z.-Y. Sun, Phys. Rev. A **101**, 052116 (2020).

[27] J. Bao, B. Guo, H.-G. Cheng, M. Zhou, J. Fu, Y.-C. Deng, and Z.-Y. Sun, Phys. Rev. A **101**, 012110 (2020).

[28] Z.-Y. Sun, M. Wang, Y.-Y. Wu, and B. Guo, Phys. Rev. A **99**, 042323 (2019).

[29] J. M. Kosterlitz and D. J. Thouless, J. Phys. C **6**, 1181 (1973).

[30] J. M. Kosterlitz, Rev. Mod. Phys. **89**, 040501 (2017).

[31] F. D. M. Haldane, Rev. Mod. Phys. **89**, 040502 (2017).

[32] X.-G. Wen, Rev. Mod. Phys. **89**, 041004 (2017).

[33] S. B. Chung, H. Yao, T. L. Hughes, and E.-A. Kim, Phys. Rev. B **81**, 060403(R) (2010).

[34] X. S. Ye, Y. J. Liu, X. H. Zeng, and G. Wu, Sci. Rep. **5**, 17358 (2015).

[35] W. W. Cheng, Z. Z. Du, L. Y. Gong, S. M. Zhao, and J. M. Liu, Europhys. Lett. **108**, 46003 (2014).

[36] A. Kitaev and J. Preskill, Phys. Rev. Lett. **96**, 110404 (2006).

[37] K. Kato, F. Furrer, and M. Murao, Phys. Rev. A **93**, 022317 (2016).

[38] A. Hamma, W. Zhang, S. Haas, and D. A. Lidar, Phys. Rev. B **77**, 155111 (2008).

[39] M. den Nijs and K. Rommelse, Phys. Rev. B **40**, 4709 (1989).

[40] H. Tasaki, Phys. Rev. Lett. **66**, 798 (1991).

[41] X.-Y. Feng, G.-M. Zhang, and T. Xiang, Phys. Rev. Lett. **98**, 087204 (2007).

[42] H. T. Wang, B. Li, and S. Y. Cho, Phys. Rev. B **87**, 054402 (2013).

[43] J. H. Liu and H. T. Wang, Eur. Phys. J. B **88**, 256 (2015).

[44] D.-L. Deng, C. Wu, J.-L. Chen, S.-J. Gu, S. Yu, and C. H. Oh, Phys. Rev. A **86**, 032305 (2012).

[45] Z.-Y. Sun, M. Li, L.-H. Sheng, and B. Guo, Phys. Rev. A **103**, 052205 (2021).

[46] R. Orús, Ann. Phys. **349**, 117 (2014).

[47] N. D. Mermin, Phys. Rev. Lett. **65**, 1838 (1990).

[48] A. V. Belinskiǐ and D. N. Klyshko, Phys. Usp. **36**, 653 (1993).

[49] B. P. Lanyon, M. Zwerger, P. Jurcevic, C. Hempel, W. Dür, H. J. Briegel, R. Blatt, and C. F. Roos, Phys. Rev. Lett. **112**, 100403 (2014).

[50] R. F. Werner and M. M. Wolf, Phys. Rev. A **64**, 032112 (2001).

[51] G.-H. Liu, W.-L. You, W. Li, and G. Su, J. Phys.: Condens. Matter **27**, 165602 (2015).

[52] I. P. McCulloch and M. Gulácsi, Europhys. Lett. **57**, 852 (2002).

[53] F. Verstraete, J. J. García-Ripoll, and J. I. Cirac, Phys. Rev. Lett. **93**, 207204 (2004).

[54] Z.-Y. Sun, H.-L. Huang, and B. Wang, Phys. Status Solidi B **250**, 370 (2013).

[55] B. S. Shastry and B. Sutherland, Phys. Rev. Lett. **47**, 964 (1981).

[56] L. G. Marland and D. D. Betts, Phys. Rev. Lett. **43**, 1618 (1979).

[57] S. Facundo, C. Federico, and A. J. Roncaglia, Nat. Commun. **10**, 2492 (2019).

[58] C. M. Dawson and M. A. Nielsen, Phys. Rev. A **69**, 052316 (2004).

[59] S. M. Giampaolo, G. Gualdi, A. Monras, and F. Illuminati, Phys. Rev. Lett. **107**, 260602 (2011).

[60] S. Campbell and M. Paternostro, Phys. Rev. A **82**, 042324 (2010).

[61] A. Friedenauer, H. Schmitz, J. T. Glueckert, D. Porras, and T. Schaetz, Nat. Phys. **4**, 757 (2008).

[62] M. Johanning, A. F. Varón, and C. Wunderlich, J. Phys. B: At., Mol. Opt. Phys. **42**, 154009 (2009).

[63] D. Porras and J. I. Cirac, Phys. Rev. Lett. **92**, 207901 (2004).

[64] M. Lewenstein, A. Sanpera, V. Ahufinger, B. Damski, A. Sen(De), and U. Sen, Adv. Phys. **56**, 243 (2007).

[65] C. Zhang, C.-J. Zhang, Y.-F. Huang, Z.-B. Hou, B.-H. Liu, C.-F. Li, and G.-C. Guo, Sci. Rep. **6**, 39327 (2016).

[66] M. M. Taddei, T. L. Silva, R. V. Nery, G. H. Aguilar, S. P. Walborn, and L. Aolita, npj Quantum Inf. **7**, 69 (2021).

[67] A. Niezgoda and J. Chwedeńczuk, Phys. Rev. Lett. **126**, 210506 (2021).

[68] G. Salvatori, A. Mandarino, and M. G. A. Paris, Phys. Rev. A **90**, 022111 (2014).

[69] M. Mehboudi, A. Sanpera, and L. A. Correa, J. Phys. A: Math. Theor. **52**, 303001 (2019).

[70] M. M. Rams, P. Sierant, O. Dutta, P. Horodecki, and J. Zakrzewski, Phys. Rev. X **8**, 021022 (2018).

[71] P. Zanardi, M. G. A. Paris, and L. Campos Venuti, Phys. Rev. A **78**, 042105 (2008).

[72] L. Garbe, M. Bina, A. Keller, M. G. A. Paris, and S. Felicetti, Phys. Rev. Lett. **124**, 120504 (2020).

[73] I. Frérot and T. Roscilde, Phys. Rev. Lett. **121**, 020402 (2018).